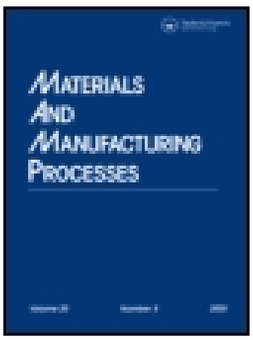

Materials and Manufacturing Processes

ISSN: 1042-6914 (Print) 1532-2475 (Online) Journal homepage: http://www.tandfonline.com/loi/lmmp20

Multi-point support technology for mirror-milling of aircraft skins

Yan Bao, Renke Kang, Zhigang Dong, Xianglong Zhu, Changrui Wang & Dongming Guo

To cite this article: Yan Bao, Renke Kang, Zhigang Dong, Xianglong Zhu, Changrui Wang & Dongming Guo (2017): Multi-point support technology for mirror-milling of aircraft skins, Materials and Manufacturing Processes, DOI: 10.1080/10426914.2017.1388519

To link to this article: http://dx.doi.org/10.1080/10426914.2017.1388519

Accepted author version posted online: 09 Oct 2017.

Submit your article to this journal

Article views: 25

View related articles

View Crossmark data

Full Terms & Conditions of access and use can be found at http://www.tandfonline.com/action/journalInformation?journalCode=lmmp20

Download by: [University of Leeds] **Date:** 24 October 2017, At: 14:40

Check for updates

Multi-point support technology for mirror-milling of aircraft skins

Yan Bao

Key Laboratory for Precision and Non-traditional Machining Technology of Ministry of Education, School of Mechanical Engineering, Dalian University of Technology, Dalian, P.R. China

Renke Kang

Key Laboratory for Precision and Non-traditional Machining Technology of Ministry of Education, School of Mechanical Engineering, Dalian University of Technology, Dalian, P.R. China

Zhigang Dong

Key Laboratory for Precision and Non-traditional Machining Technology of Ministry of Education, School of Mechanical Engineering, Dalian University of Technology, Dalian, P.R. China

Xianglong Zhu

Key Laboratory for Precision and Non-traditional Machining Technology of Ministry of Education, School of Mechanical Engineering, Dalian University of Technology, Dalian, P.R. China

Downloaded by [University of Leeds] at 14:40 24 October 2017

Accepted Manuscript

Changrui Wang

Key Laboratory for Precision and Non-traditional Machining Technology of Ministry of Education, School of Mechanical Engineering, Dalian University of Technology, Dalian, P.R. China

Dongming Guo

Key Laboratory for Precision and Non-traditional Machining Technology of Ministry of Education, School of Mechanical Engineering, Dalian University of Technology, Dalian, P.R. China

Address correspondence to Zhigang Dong, Key Laboratory for Precision and Non-traditional Machining Technology of Ministry of Education, School of Mechanical Engineering, Dalian University of Technology, No. 2 Linggong Rd, Dalian 116024, P.R. China. E-mail: dongzg@dlut.edu.cn

Downloaded by [University of Leeds] at 14:40 24 October 2017

Accepted Manuscript

ABSTRACT

Mirror milling is a new efficient and green technology of aircraft skin processing. Currently, the support head of mirror milling system is mostly a metallic sphere and the support area is smaller than the milling area, which results in the deformation error of workpiece. In order to solve this problem, a new multi-point support device is proposed. The purpose of this research is to optimize the support location of multi-point support in mirror milling of aircraft skin parts. The simulation and experimental studies indicate that: the deformation of the workpiece is reduced by increasing the support points. In order to obtain the good thickness consistency of workpiece, the distribution of the support points should make the rigidity distribution of the workpiece consistent

with the change of milling force, not as close as the milling trajectory. The workpiece deformation error can be reduced only by changing the support locations.

KEYWORDS: aircraft, deformation, distribution, location, milling, optimization, skin, support

Downloaded by [University of Leeds] at 14:40 24 October 2017

Accepted Manuscript

Introduction

Aircraft skins form the aircraft aerodynamic configuration which require low damage and high accuracy[1]. Aircraft skin parts are characterized with low rigidity, large size, thin floor structure, and complex shape[2–5]. There are single curvature parts, double curvature parts, and even more complex shape parts among skin parts. Sometimes the curvature of skin surface varies gradually[6]. For aerospace products, it is very important to reduce the weight, which drives skin panels the thinner the better[7]. Nowadays, skins are generally monolithic structures rather than many small parts which are joined by welding or riveting[8]. The final part is obtained from an initial raw block, in which the 90–95% of material is removed[3]. Currently, chemical milling is commonly used to reduce the thickness of aircraft skins, which unfortunately is not environmentally friendly[9,10]. Furthermore, the process is long and complicated[11–13]. Also, large energy consumption is a big problem[14]. Accordingly, it has become more prominent to find a new environmentally friendly process to replace chemical milling.

For solving these issues, mirror milling system (MMS) is proposed for machining aircraft skins, which is currently applied in Airbus Company[15,16]. MMS includes two five-axis machines used on the two sides of a skin part moving synchronously. The first one performs the pocket milling, and the other support on the opposite side. The support head is usually a metallic

sphere[7,12,17,18]. MMS gradually becomes the next generation machining technology for aircraft skin, used to replace chemical milling[14].

Because of the advantage in thickness reduction of thin and large aircraft skin parts, MMS has attracted wide attention. A lot of researches have been carried out not only in the equipment development[7,19–32] but also in process technology. However, to the authors' knowledge, process technology has been less studied than device development. Mahmud at University of Montreal developed a machining end effector used for mirror-milling and established a milling force model considering the influence of the angle of the spindle in order to determine the minimum clamping force, and presented a master-to-slave motion transfer function by only considering the lateral sliding motion[33,34]. Li and his team proposed a feature-based method for mirror-milling broken surfaces[35,36]. A stiffness model for a mirror milling device was established by Wang et al.[37,38] Xiao and his team proposed a means of mirror-milling aircraft skin and optimizing the moving path of support head[39]. However, this system is not the same with the previously mentioned MMS in mechanism because the two support heads didn't move on the same vector direction. Bao at Dalian University of Technology proposed a cutting force model for MMS and presented the fluid lubricating support method used to reduce the scratches of aircraft skin surface. The influence of parameter of liquid film on processing quality of workpiece were studied[40,41]. In MMS, the support head is usually a metallic sphere and its support area is much smaller than the milling area, resulting in workpiece elastic deformation during milling. So the profile error of the workpiece can be reduced by optimizing the support location[42]. One could easily argue that workpiece elastic deformation will be decreased by adding support points. However, there are two problems to confront: how many support points to increase and where to set the support points. The purpose of this research is to solve these two problems which have not yet been intensively studied.

Downloaded by [University of Leeds] at 14:40 24 October 2017

Accepted Manuscript

The paper focuses on the optimization of support location of multi-point support in mirror milling of aircraft skin parts. The rest of the paper is organized as follows: Section 2 proposed a workpiece deformation prediction model and optimized support location of multi-point support in mirror-milling; the experimental analysis and verification at different support locations are discussed in Section 3; and the final conclusions are drawn in Section 4.

Materials and methods

During mirror milling aircraft skins, the two heads are on the same vector along the normal direction of the workpiece, so the distance between the two heads is equal to the machined skin thickness[12]. However, because of the low rigidity of the workpiece in tool axial direction, the workpiece will deform mainly in the tool axial direction of the cutting zone. The workpiece thickness error is mainly affected by the tool axial deformation, and therefore the workpiece deformation only in tool axial direction is considered in the paper.

Milling force model

An extensive research has been carried out on modelling of milling force, which can be roughly divided into empirical, analytical, mechanistic, and numerical models[43–50]. Among them, the mechanistic model is widely used because of the superiorities in experimental workload and predictive accuracy[51]. It is customary to define the milling forces mechanistically as a function of milling conditions and the milling constants and as follows[52]:

$$\begin{aligned} dF_{\mathrm{t}} &= K_{\mathrm{te}} dL + K_{\mathrm{tc}} s\, dz \\ dF_{\mathrm{r}} &= K_{\mathrm{re}} dL + K_{\mathrm{rc}} s\, dz \\ dF_{\mathrm{a}} &= K_{\mathrm{ae}} dL + K_{\mathrm{ac}} s\, dz \end{aligned} \qquad (1)$$

Downloaded by [University of Leeds] at 14:40 24 October 2017

Accepted Manuscript

with dL the elementary length of the cutting edge, s the uncut chip thickness, and dz the elementary height of the cutting edge. dF_t, dF_r, and dF_a represent tangential force, radial force and axial force respectively. Parameters K_{te}, K_{re}, K_{ae}, K_{tc}, K_{rc}, K_{ac} are the milling force coefficients, which are directly calibrated from metal cutting experiments for a tool-workpiece pair. The detailed description of the process are reported in previous work[42]. In the milling force coefficient calibration experiment, a DEREK EMR-20-4R20-160-2T abandon bull nose milling cutter with 20mm diameter was applied, on which one RPMT08T2M0E-JS VP15TF cemented carbide insert from Mitsubishi was fixed. Aluminum alloy 7075 was used as workpiece material. From 200 to 400m /min, every 50m /min was taken as the speed of cut. The feed per tooth was every 0.05mm from 0.05 to 0.25mm while the axial cutting depth was every 0.05mm from 0.1 to 0.3mm . The verification experiment was conducted under the conditions of milling speed 325m /min, feed per tooth 0.12mm and axial cutting depth 0.2mm . The predicted and measured milling forces are in good agreement.

Finite element analysis

In MMS, the workpiece thickness error is greatly affected by the workpiece elastic deformation. Finite element method (FEM) is commonly used to predict and analyze the deformation of low rigidity components[53–56]. Therefore, FEM has been used to calculate the deformation value in this study. Whether the array suction cups or the surrounding holders, as flexible fixtures, are used to fix the periphery of the workpiece, which is far away from the work region, the distance between the fixed point and the support point is much larger than that between the cutting force point and the support point[12,19]. Thus, in the finite element simulation, some system assumptions are set as the same as that in the previous work[42].

Downloaded by [University of Leeds] at 14:40 24 October 2017

Accepted Manuscript

Based on the above assumptions, the aircraft skin part is assumed to be a 500mm diameter circular 7075 aluminum alloy plate for simplification (**Figure 1**). Taking fine finishing as an example, the initial skin thickness was 1mm, the axial cutting depth 0.2mm, and the radial cutting depth 6mm, and the predicted milling forces were used for FEA. The support point was simplified to a steel ball with the same diameter. Both the periphery of the workpiece and the steel ball were fixed. The sweep angle of cutter ($\theta_s = \theta_{ex} - \theta_{en}$) was divided into 10 parts in which θ_{ex} and θ_{en} were exit angle and entrance angle respectively. Each instantaneous milling force was applied to the corresponding point of workpiece. An FE model of workpiece deformation was developed.

Optimization of support location

During mirror milling aircraft skins, the two heads are on the same vector along the normal direction of the workpiece. However, the supported area is smaller than the milling area, which can result in workpiece elastic deformation during milling. The milling forces vary in the direction of the milling tool axis, which may also produce different workpiece deformation along Y direction (**Figure 2**).

It is easy to understand that increasing the number of support points will result in improving the rigidity of cutting area and reducing the workpiece deformation. However, aircraft skin is a typical complex shape part, which is usually double curved. Therefore, in order to adapt to the change of curvature, the maximum number of support points is three at the same time. So the distribution of support points is optimized when the support head are respectively one-point, two-point, and three-point. In the direction of the entrance point and the exit point from the original support point, 4 equal parts are taken with 2×2 mm^2 per part and the matrix of support location is established and shown in **Figure 3**. The deformation of workpiece at each support location or each

Downloaded by [University of Leeds] at 14:40 24 October 2017

Accepted Manuscript

support location combination (for multi-point support) is calculated by FEM, and the statistical results of the dimensional error of the workpiece floor thickness are illustrated in **Figure 4**.

As shown in **Figure 4**, with the number of support points increasing, the average and minimum values of dimensional error caused by elastic deformation decreases gradually. However, the maximum error decreasing is not that obvious. This is because, even if the number of support points is increased, the positions of the support points are concentrated in the places where the force is minimum, so that there is not a significant effect on decreasing the maximum deformation. When milling thin floor workpiece, the thickness error of workpiece is an important factor to evaluate the workpiece dimensional accuracy. However, the variation of the workpiece thickness error in the radial cutting width is difficult to be reduced by the compensation method. In order to reduce the variation of thickness error, two feasible methods is to reduce the radial cutting width or the axial cutting depth, so as to reducing the variation of milling forces. But these two methods greatly reduce the processing efficiency. Therefore, the consistency of workpiece thickness is regarded as the main factor to evaluate the dimensional accuracy of the workpiece by mirror-milling in this study. The results of the worst and best consistency of workpiece thickness, which means the maximum and minimum deformation fluctuation, are shown in **Figure 5**, when the support head are respectively one-point, two-point, and three-point.

As shown in **Figure 5a, c, e**, the worst surface profiles are similar whether the support head is one-point, two-point, or three-point. And the locations of the support points are concentrated in the entrance point of the milling trajectory. This is because: in order to get large deformation fluctuation, it is necessary to make the rigidity of workpiece lowest in the place where the milling force is largest and the rigidity of workpiece highest in the place where the milling force is

Downloaded by [University of Leeds] at 14:40 24 October 2017

Accepted Manuscript

smallest. If small deformation fluctuation is wanted, just opposite the workpiece rigidity distribution. Therefore, the support points are concentrated in the vicinity of the entrance point. As shown in **Figure 5b, d, f**, increase the support points will result in reducing the deformation of the workpiece. However, the optimal support location is not near the milling trajectory. The intuitive feeling is that the support point is closer to the milling trajectory, the deformation of the workpiece is smaller. That's right, however, in order to make the thickness consistency of the workpiece best, the distribution of the support points should make the rigidity distribution of the workpiece consistent with the change of milling force, not as close as the milling trajectory.

Results and discussion

Experiments were conducted on the test rig shown in **Figure 6** to verify the validity of the optimization results. In the experiment setup, a two-dimensional horizontal moving platform (**Figure 6a**) and a support device (**Figure 6b**) were installed on the workbench of the three-axis vertical milling machine. The support device was composed of a lifting platform and interchangeable rectangular plates embedded balls in various location that was mounted on the workbench. The workpiece was clamped on a large frame which was mounted on the two dimensional horizontal moving platform. During processing, the axes of the milling tool and the support device were on the same vector, and the cutting tool was fed to a limited distance (the nominal thickness of the skin). The feed motion was realized through the movement of the workpiece. The cutting tool, workpiece materials and cutting parameters were the same as those in the aforementioned milling force coefficient calibration verification experiment.

As the workpiece is clamped on a large frame, the workpiece rigidity varies in different positions, the workpiece produces different deformation in different positions under the same

Downloaded by [University of Leeds] at 14:40 24 October 2017

Accepted Manuscript

cutting parameters. Thus, only the deformation of the workpiece center was measured for comparision. After milling, the actual thickness of the workpiece was measured by two displacement laser sensors (Keyence, LK-H025), which were placed face to face in the opposite directions (**Figure 7**). During measuring, the two displacement laser sensors are fixed, while the workpiece is moved horizontally by the two dimensional horizontal moving platform. The thickness changes of the workpiece can be obtained by adding the data measured by the two sensors. So the thickness of the machined workpiece can be calculated by measuring the thickness of the uncut workpiece.

Although the fixturing methods of the workpiece are different in the experiment and MMS, the deformation laws for the middle work area of the workpiece in both the experiment and MMS are the same, resulting in little difference in deformation. The verification experiment was performed. The measured surface profiles of workpiece at different support coordinates were shown in **Figure 8**.

Comparing the predicted (**Figure 5**) and measured (**Figure 8**) results, it's indicated that they are in a good agreement not only in shape but also in magnitude. The simulation system meets the anticipated request. The deformation fluctuation of three-point support is smallest among these three kinds of support head. The measured profile height difference of workpiece E (**Figure 8e**) is 49.4 μm, while that of workpiece F (**Figure 8f**) is 10.2 μm. That is to say, compared with the deformation fluctuation due to the support at location E that at location F is decreased by 79.4%.

Because the workpiece and the tool are not rigid body, they will inevitably deform under the influence of the milling forces. In MMS, the workpiece rigidity is much smaller than that of the tool. Thus, the workpiece deformation is the main factor of the workpiece thickness error. The

Downloaded by [University of Leeds] at 14:40 24 October 2017

Accepted Manuscript

workpiece deformation is determined by the milling forces and the workpiece rigidity. Therefore, in the case of no change of cutting parameters, what can be changed is only the rigidity of the workpiece to control the deformation of the workpiece. By changing the support point location, the distribution of the rigidity of the workpiece surface is consistent with the change of milling forces. Thus, the purpose of controlling the workpiece deformation fluctuation can be achieved. The consistency of the remaining wall thickness after processing is improved, and the machining error is reduced.

Downloaded by [University of Leeds] at 14:40 24 October 2017

Conclusions

The multi-point support technology and optimization of support location of multi-point support in mirror-milling is presented in this study. In addition, a new multi-point support device used to verify the optimized support location of multi-point support in mirror milling of aircraft skin parts is proposed. When the support head is respectively one-point, two-point, and three-point, the maximum and minimum deformation fluctuation of workpiece is predicted and experimental verified. The results show that: the deformation of the workpiece is reduced by increasing the support points. In order to make the thickness consistency of the workpiece best, the distribution of the support points should make the rigidity distribution of the workpiece consistent with the change of milling force, not as close as the milling trajectory. The profile height difference of workpiece is decreased and flat surface topographies are obtained by changing the support head location.

Accepted Manuscript

Funding

This research was supported by the Science Fund for Creative Research Groups of NSFC (grant number 51621064); the Science Challenge Project (grant number JCKY2016212A506-0103); and the National Engineering and Research Center for Commercial Aircraft Manufacturing (grant number 201500308).

References

[1] He, D.; Li, X.; Li, D.; Yang, W. Process Design for Multi-Stage Stretch Forming of Aluminium Alloy Aircraft Skin. *Trans. Nonferrous Metals Soc. China* **2010**, *20*(6), 1053–1058. DOI: 10.1016/S1003-6326(09)60257-0.

[2] Campa, F. J.; Lopez de Lacalle, L. N.; Celaya, A. Chatter Avoidance in the Milling of Thin Floors with Bull-Nose End Mills: Model and Stability Diagrams. *Int. J. Mach. Tools Manuf.* **2011**, *51*(1), 43–53. DOI: 10.1016/j.ijmachtools.2010.09.008.

[3] Herranz, S.; Campa, F. J.; Lopez de Lacalle, L. N.; Rivero, A.; Lamikiz, A.; Ukar, E.; Sanchez, J. A.; Bravo, U. The Milling of Airframe Components with Low Rigidity: A General Approach to Avoid Static and Dynamic Problems. *Proc. Inst. Mech. Eng. Part B J. Eng. Manuf.* **2005**, *219*, 789–801. DOI: 10.1243/095440505X32742.

[4] Han, Z.; Dai, L.; Zhang, L. Current Status of Large Aircraft Skin and Panel Manufacturing Technologies. *Aeronaut. Manuf. Technol.* **2009**, *4*, 64–66. DOI: 10.3969/j.issn.1671-833X.2009.04.007.

[5] Zhou, K. Flexible Tooling and Fixture Technology of large Thin-Wall Part Manufacturing for Aircraft. *Aeronaut. Manuf. Technol.* **2012**, *3*, 34–39. DOI: 10.3969/j.issn.1671-833X.2012.03.003.

[6] Zhou, G.; Li, Y.; Liu, C.; Hao, X. A Feature-Based automatic Broken Surfaces Fitting Method for Complex Aircraft Skin Parts. *Int. J. Adv. Manuf. Technol.* **2016**, *84*(5), 1001–1011. DOI: 10.1007/s00170-015-7774-y.

[7] Mahmud, A. Mechanical Pocket Milling of Thin Aluminum Panel with a Grasping and Machining End Effector. Dissertation, Universite De Montreal, 2015.

[8] Campa, F. J.; Lopez de Lacalle, L. N.; Herranz, S.; Lamikiz, A.; Rivero, A. Avoiding Instability on the Milling of Parts with Thin Features. *Mater. Sci. Forum* **2006**, *526*, 37–42. DOI: 10.4028/www.scientific.net/MSF.526.37.

[9] Moradi, H. Optimization of Cutting Parameters for Pocket Milling on the Skin Plate in Al and Al-Li Materials. Dissertation, Universite De Montreal, 2014.

[10] Cakir, O.; Yardimeden, A.; Ozben, T. Chemical Machining. *Arch. Mater. Sci. Eng.* **2007**, *28*(8), 499–502.

[11] Lin, C.; Cai, J.; Zeng, F.; Huang, X.; Du, N.; Zhao, Q. Chemical Milling Technology and Influencing Factors of Processing Quality of LY12 Aluminum Alloy. *Failure Anal. Prev.* **2010**, *5*(1), 8–12, 16. DOI: 10.3969/j.issn.1673-6214.2010.01.003.

[12] Panczuk, R.; Foissac, P. Y. Process and a Device for the Machining of Panels. US Patent 7682112, B2, 2010.

Downloaded by [University of Leeds] at 14:40 24 October 2017

Accepted Manuscript

[13] Jin, Y. Design of Equipment for Chemical Milling of Rocket Tank Sheets. *Missile Space Veh.* **2009**, *2*, 52–56. DOI: 10.3969/j.issn.1004-7182.2009.02.013.
[14] Lu, D. New Generation Green Machining Technology for Aircraft Skin. *Aeronaut. Manuf. Technol.* **2010**, *16*, 102–103. DOI: 10.3969/j.issn.1671-833X.2010.16.024.
[15] Zhang, Z.; Xu, X. MMS: The Latest Green Skin Machining System. *Aeronaut. Manuf. Technol.* **2010**, *19*, 84–86. DOI: 10.3969/j.issn.1671-833X.2010.19.011.
[16] Zhang, X.; Duan, X. Flexible Champing and CNC Milling Technology of Aircraft Skin. *Aeronaut. Manuf. Technol.* **2015**, *S1*, 42–44. DOI: 10.16080/j.issn1671-833x.2015.S1.042.
[17] Xu, M.; Xiang, B.; Li, X.; Wang, Y.; Lan, H. Application of Mirror Milling System and Advanced Machining Technology for Aircraft Skin. *Manuf. Technol. Mach. Tool* **2014**, *11*, 40–43. DOI: 10.3969/j.issn.1005-2402.2014.11.016.
[18] Xiang, B.; Huang, J.; Xu, J.; Zhou, X.; Li, Y.; Hao, X. Mirror Top Bracing Technology in Milling Aircraft Skin. *Manuf. Technol. Mach. Tool* **2015**, *4*, 92–96. DOI: 10.3969/j.issn.1005-2402.2015.04.023.
[19] Martinez, M. T.; Fuerte, S. E. Machine Tool Installation for Supporting and Machining Workpieces. US Patent, 5163793, 1992.
[20] Hamann, J. C.; Baule, L. Process and Device for Machining by Windowing of Non-deformable Thin Panels. US Patent 7168898 B2, 2007.
[21] Li, Y.; Hao, X.; Zhou, X.; Mu, W.; Tang, L. Process and a Device for the Mirror Milling of Aircraft Skin. China Patent 104400086B, 2016.
[22] Li, Y.; Hao, X.; Ma, S.; Zhou, X.; Zhao, X.; Mu, W.; Tang, L. Process and a Device for the Support of Mirror Milling of Aircraft Skin. China Patent 104440158B, 2016.
[23] Li, Y.; Hao, X.; Chen, G.; Zhou, X. Adaptive Adsorption and Clamping Device for Aircraft Skin. China Patent 104647090B, 2016.
[24] Li, Y.; Hao, X.; Zhou, G.; Zhou, X.; Mu, W.; Tang, L. Adaptive Processing of Skin Based on Laser Displacement Sensors. China Patent 104385052B, 2016.
[25] Li, Y.; Hao, X.; Ma, S.; Zhou, X.; Zhao, X.; Mu, W.; Tang, L. Process and a Testing Device for the Real Time Adaptive Mirror Milling Based on Multi Sensor. China Patent 104476321B, 2016.
[26] Wang, H.; Zhao, Y.; Chen, G.; Lai, X.; Hao, J. A Parallel Rotational-Translational Decoupling Processing Equipment for Thin-Walled Part Milling. China Patent 104001974B, 2016.
[27] Wang, H.; Zhao, Y.; Chen, G.; Lai, X.; Hao, J. Multi Point Flexible Rolling Support Head for Mirror Processing Equipment. China Patent 104002161B, 2016.
[28] Xiao, J.; Yao, Y.; Huang, T.; Lin, B.; Ji, J. Sucking Support Head Provided with Rigid and Flexible Supports and Used for Machining Grids of Thin-Walled Workpiece. China Patent 104690577B, 2017.
[29] Xiao, J.; Yao, Y.; Huang, T.; Lin, B.; Ji, J.; Zhang, X.; Lin, B. Hard-Soft Multipoint Follow-Up Support Head Used for Image Processing. China Patent 14668989B, 2016.
[30] Wang, Q.; Wang, Y.; Ding, P.; Bi, Q.; Sun, X.; Liu, G.; Chen, W. Multi Head Mirror Milling Device for Barrel Shaped Thin-Wall Workpiece. China Patent 104400093B, 2015.
[31] Wang, Q.; Ding, P.; Wang, Y.; Sun, X.; Bi, Q.; Huang, C.; Liu, S.; Chen, W.; Tian, T.; Xu, Y.; Li, X. Integral Manufacturing Method of Large Storage Tank Section Based on Numerical Control Milling. China Patent 104439968B, 2015.

Downloaded by [University of Leeds] at 14:40 24 October 2017

Accepted Manuscript

[32] Wang, Q.; Ding, P.; Sun, X.; Li, Y.; Liu, G.; Liu, S.; Chen, W. Dual Channel Coordinated Motion Control Method for Mirror Milling. China Patent 104360636B, 2016.
[33] Mahmud, A.; Mayer, J. R. R.; Baron, L. Determining the Minimum Clamping Force by Cutting Force Simulation in Aerospace Fuselage Pocket Machining. *Int. J. Advanced Manuf. Technol.* **2015**, *80*(9), 1751–1758. DOI: 10.1007/s00170-015-7104-4.
[34] Mahmud, A.; Mayer, J. R. R.; Baron, L. Magnetic Attraction Forces Between Permanent Magnet Group Arrays in a Mobile Magnetic Clamp for Pocket Machining. *CIRP J. Manuf. Sci. Technol.* **2015**, *11*, 82–88. DOI: 10.1016/j.cirpj.2015.08.005.
[35] Liu, S.; Li, Y.; Hao, X.; Liu, C.; Xiang, B. Feature-Based Uncut Region Tool Path Optimization Method for Skin Parts Machined by Mirror Milling System. *Acta Aeronaut. Astronaut. Sin.* **2016**, *37*(7), 2295–2302. DOI: 10.7527/S1000-6893.2015.0240.
[36] Hu, M.; Xiang, B.; Li, Y.; Xu, M.; Zhu, X. Application of Feature-Based Rapid Programming Technology for Aircraft Panels. *Manuf. Technol. Mach. Tool* **2016**, *1*, 148–152. DOI: 10.3969/j.issn.1005-2402.2016.01.041.
[37] Hao, J.; Zhao, Y.; Wang, H.; Sheng, D. Synthetical Stiffness Analysis and Optimization of Mirror Support Mechanism for Thin-Walled Structures. *Mach. Des. Res.* **2015**, *31*(2), 155–159, 163.
[38] Zhao, Y.; Wang, Z.; Wang, H.; Hao, J.; Yu, D. Stiffness Analysis and Optimization of Supporting Mechanism Based on Tricept for Thin-Walled Part Milling System. The 14th IFToMM World Congress, Taipei, Taiwan, 25–30 October 2015. DOI: 10.6567/IFToMM.14TH.WC.OS13.075.
[39] Lan, J.; Lin, B.; Huang, T.; Xiao, J.; Zhang, X.; Fei, J. Path Planning for Support Heads in Mirror-Milling Machining System. *Int. J. Adv. Manuf. Technol.* **2016**, 1–12. DOI: 10.1007/s00170-016-9725-7 (in press).
[40] Bao, Y.; Dong, Z.; Kang, R.; Li, Z.; Yuan, Y. Milling Force and Machining Deformation in Mirror Milling of Aircraft Skin. *Adv. Mater. Res.* **2016**, *1136*, 149–155. DOI: 10.4028/www.scientific.net/AMR.1136.149.
[41] Li, Z.; Bao, Y.; Kang, R.; Dong, Z.; Zhou, P.; Jin, Z. An Advanced Support Method of Aircraft Skin Mirror Milling - Fluid Lubricating Support. *Mater. Sci. Forum* **2016**, *874*, 469–474. DOI: 10.4028/www.scientific.net/MSF.874.469.
[42] Bao, Y.; Zhu, X.; Kang, R.; Dong, Z.; Zhang, B.; Guo, D. Optimization of Support Location in Mirror-Milling of Aircraft Skins. *Proc. Inst. Mech. Eng. Part B J. Eng. Manuf.* **2016**, 1–8. DOI: 10.1177/0954405416673110 (in press).
[43] Altintas, Y. *Manufacturing automation: metal cutting mechanics, machine tool vibrations, and CNC design*, 2nd ed.; Cambridge University Press: New York, 2012.
[44] Nakayama, K.; Arai, M.; Takei, K. Semi-Empirical Equations for Three Components of Resultant Cutting Force. *CIRP Ann. Manuf. Technol.* **1983**, *32*(1), 33–35. DOI: 10.1016/S0007-8506(07)63356-3.
[45] Aydin, M.; Ucar, M.; Cengiz, A.; Kurt, M.; Bakir, B. A Methodology for Cutting Force Prediction in Side Milling. *Mater. Manuf. Process* **2014**, *29*(11–12), 1429–1435. DOI: 10.1080/10426914.2014.912315.
[46] Oxley, P. L. B. *Mechanics of Machining: An Analytical Approach to Assessing Machinability*; Ellis Horwood: Chichester, 1989.

Downloaded by [University of Leeds] at 14:40 24 October 2017

Accepted Manuscript

[47] Khajehzadeh, M.; Razfar, M. R. FEM and Experimental Investigation of Cutting Force During UAT Using Multicoated Inserts. *Mater. Manuf. Process* **2015**, *30*(7), 858–867. DOI: 10.1080/10426914.2014.973590.
[48] Bajpai, V.; Lee, I.; Park, H. W. Finite Element Modeling of Three-Dimensional Milling Process of Ti-6Al-4V. *Mater. Manuf. Process* **2014**, *29*(5), 564–571. DOI: 10.1080/10426914.2014.892618.
[49] Limido, J.; Espinosa, C.; Salauna, M.; Lacome, J. L. SPH Method Applied to High Speed Cutting Modelling. *Int. J. Mech. Sci.* **2007**, *49*(7), 898–908. DOI: 10.1016/j.ijmecsci.2006.11.005.
[50] Jin, X.; Altintas, Y. Slip-Line Field Model of Micro-Cutting Process with Round Tool Edge Effect. *J. Mater. Process. Technol.* **2011**, *211*(3), 339–355. DOI: 10.1016/j.jmatprotec.2010.10.006.
[51] Budak, E.; Altintas, Y.; Armarego, E. J. A. Prediction of Milling Force Coefficients from Orthogonal Cutting Data. *Trans. ASME J. Manuf. Sci. Eng.* **1996**, *118*(2), 216–224. DOI: 10.1115/1.2831014.
[52] Arnaud, L.; Gonzalo, O.; Seguy, S.; Jauregi, H.; Peigne, G. Simulation of Low Rigidity Part Machining Applied to Thin-Walled Structures. *Int. J. Adv. Manuf. Technol.* **2011**, *54*(5–8), 479–488. DOI: 10.1007/s00170-010-2976-9.
[53] Ratchev, S.; Liu, S.; Huang, W.; Becher, A. A. An Advanced FEA Based Force Induced Error Compensation Strategy in Milling. *Int. J. Mach. Tools Manuf.* **2006**, *46*(5), 542–551. DOI: 10.1016/j.ijmachtools.2005.06.003.
[54] Gao, Y.; Ma, J.; Jia, Z.; Wang, F.; Si, L.; Song, D. Tool Path Planning and Machining Deformation Compensation in High-Speed Milling for Difficult-to-Machine Material Thin-Walled Parts with Curved Surface. *Int. J. Adv. Manuf. Technol.* **2016**, *84*(9–12), 1757–1767. DOI: 10.1007/s00170-015-7825-4.
[55] Li, A.; Pang, J.; Zhao, J.; Zang, J.; Wang, F. FEM-Simulation of Machining Induced Surface Plastic Deformation and Microstructural Texture Evolution of Ti-6Al-4V Alloy. *Int. J. Mech. Sci.* **2017**, *123*, 214–223. DOI: 10.1016/j.ijmecsci.2017.02.014.
[56] Bhattacharya, A.; Bera, T. K.; Thakur, A. On Cutter Deflection Profile Errors in End Milling: Modeling and Experimental Validation. *Mater. Manuf. Process* **2015**, *30*(8), 1042–1050. DOI: 10.1080/10426914.2014.973598.

Downloaded by [University of Leeds] at 14:40 24 October 2017

Accepted Manuscript

Figure 1. Schematic of cutting zone for the FE model of mirror-milling the skin panel.

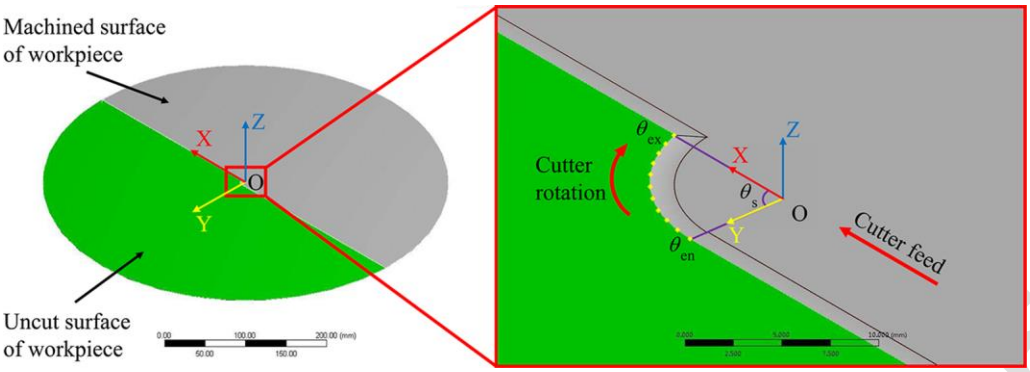

Downloaded by [University of Leeds] at 14:40 24 October 2017

Accepted Manuscript

Figure 2. Section view in plane OYZ.

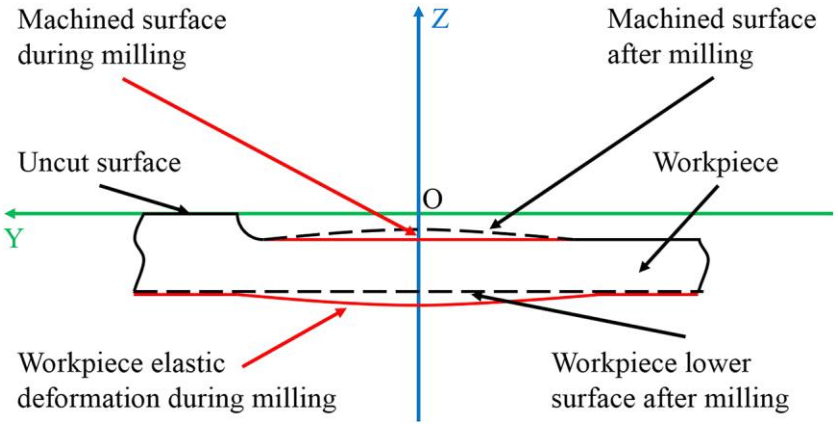

Downloaded by [University of Leeds] at 14:40 24 October 2017

Accepted Manuscript

Figure 3. Supporting locations in the FEM calculation.

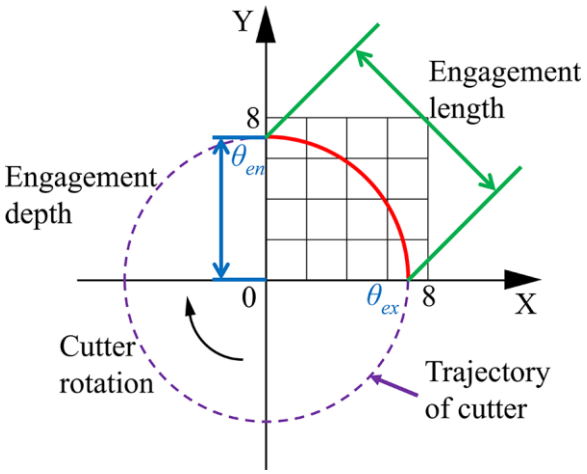

Downloaded by [University of Leeds] at 14:40 24 October 2017

Accepted Manuscript

Figure 4. The influence of the number of support points on the dimensional error.

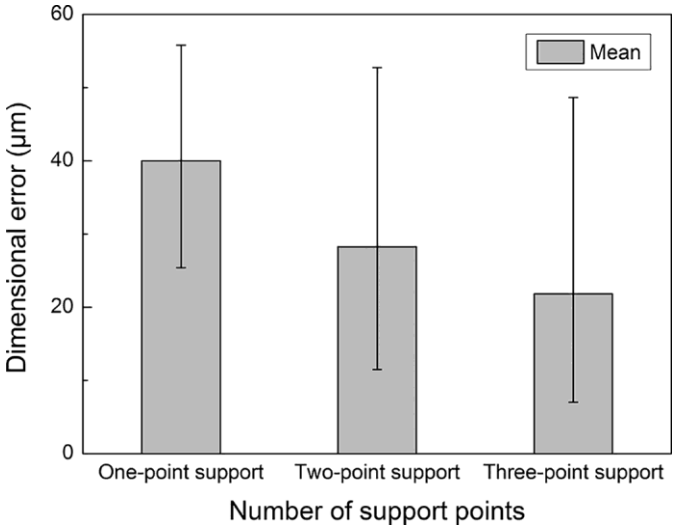

Downloaded by [University of Leeds] at 14:40 24 October 2017

Accepted Manuscript

Figure 5. Predicted surface profiles of workpiece at some representative support locations.

	One-point support	Two-point support	Three-point support
Worst	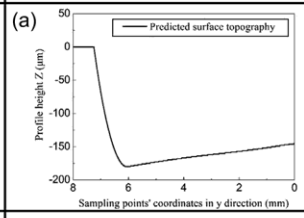	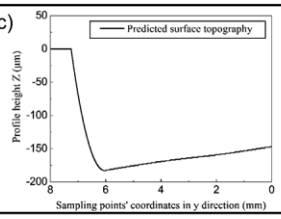	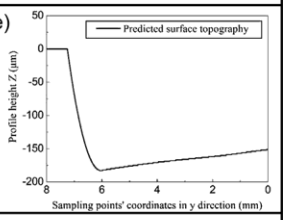
Support coordinates	(x=0, y=8)	(x=0, y=6) (x=0, y=8)	(x=0, y=4) (x=0, y=6) (x=0, y=8)
Best	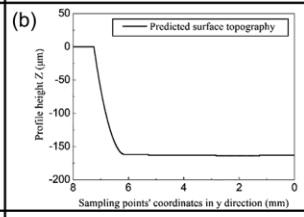	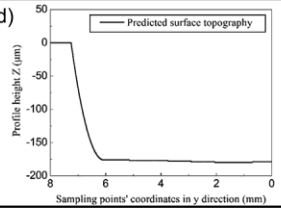	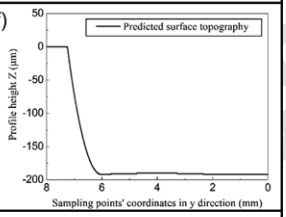
Support coordinates	(x=2, y=0)	(x=2, y=2) (x=4, y=0)	(x=0, y=4) (x=6, y=0) (x=6, y=8)

Downloaded by [University of Leeds] at 14:40 24 October 2017

Accepted Manuscript

Figure 6. Experimental platform: (a) two dimensional horizontal moving platform, (b) supporting device.

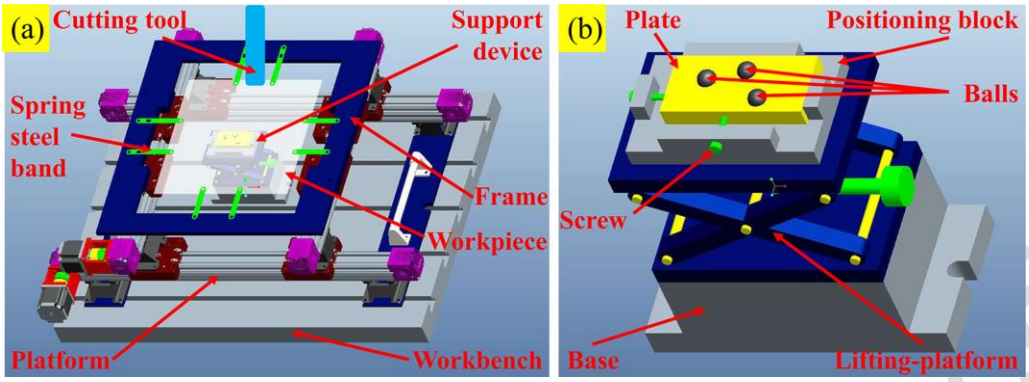

Downloaded by [University of Leeds] at 14:40 24 October 2017

Accepted Manuscript

Figure 7. Thickness measurement device with two laser displacement sensors.

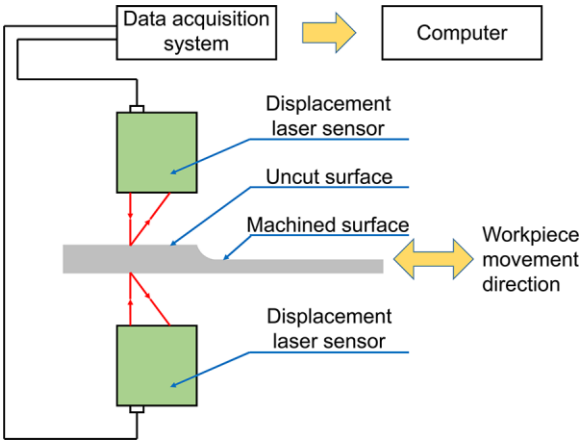

Downloaded by [University of Leeds] at 14:40 24 October 2017

Accepted Manuscript

Figure 8. Measured surface profiles of workpiece at the support coordinates.

	One-point support	Two-point support	Three-point support
Worst	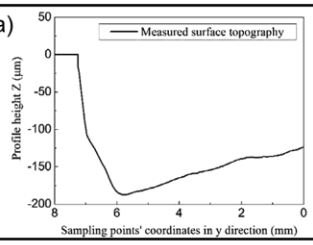	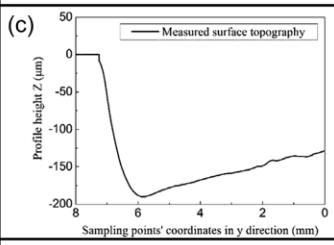	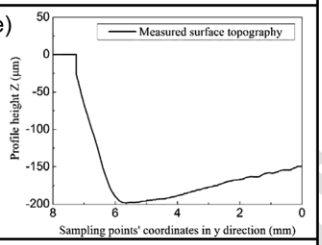
Support coordinates	(x=0, y=8)	(x=0, y=6) (x=0, y=8)	(x=0, y=4) (x=0, y=6) (x=0, y=8)
Best	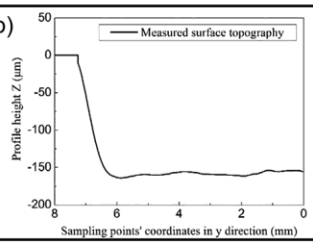	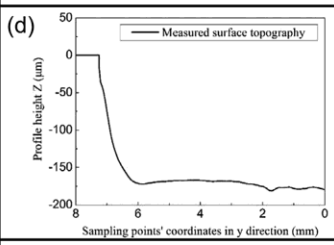	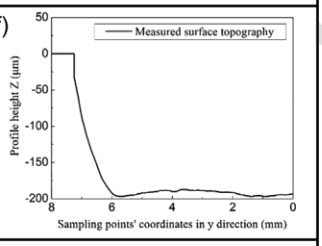
Support coordinates	(x=2, y=0)	(x=2, y=2) (x=4, y=0)	(x=0, y=4) (x=6, y=0) (x=6, y=8)

Downloaded by [University of Leeds] at 14:40 24 October 2017

Accepted Manuscript